Numerical study of positron-hydrogen scattering

Larkin, J. M; Eberly, J. H; Lappas, D. G; Grobe, R

Published in:
Physical Review A (Atomic, Molecular and Optical Physics)

DOI:
10.1103/PhysRevA.57.2572

1998

Numerical study of positron-hydrogen scattering

J. M. Larkin and J. H. Eberly
Department of Physics and Astronomy, University of Rochester, Rochester, New York 14627

D. G. Lappas
Department of Physics, Lund Institute of Technology, P.O. Box 118, S-221 00, Lund, Sweden

R. Grobe
Intense Laser Physics Theory Unit, Department of Physics, Illinois State University, Normal, Illinois 61790-4560
(Received 9 February 1996; revised manuscript received 30 June 1997)

We present results of numerical experiments that are the one-dimensional analog of positron-hydrogen scattering. The obtained wave functions are exact, within model restrictions. [S1050-2947(98)01501-7]

PACS number(s): 34.70.+e, 32.80.Rm, 34.50.Rk

I. INTRODUCTION

The positron-hydrogen system is one of the simplest three-particle systems in that a rearrangement process can be observed. The system consists of three distinguishable particles that can exist in three steady-state configurations: hydrogen and free positron ($H+e^+$), positronium and free proton ($Ps+p$), and three dissociated particles (e^++e^-+p). There is no positron-electron-proton bound state [1,2]. Theoretical work on this system began with the work of Massey and Mohr [3] in 1954 and it has continued to be an area of active research [4–6]. Experimentally, this has been a very difficult system to study, mainly because of the low intensities of the available positron beams. The first measurements of the positronium formation cross section were not reported until the beginning of this decade [7]. A brief review of the most recent available calculations and experimental data is given by Kernoghan *et al.* [8].

In this paper we report initial results from numerical experiments that are the one-dimensional analog of positron-hydrogen scattering. The restriction to one dimension (1D) obviously eliminates many physical effects from consideration. For example, in 1D there are only two scattering directions, forward and backward. However, the problem remains fully quantum mechanical in 1D, and we can exploit the greater simplicity to obtain numerically the exact two-body time-dependent wave functions, including the effect of the full correlation interaction without approximation. These wave functions can permit inspection of the rearrangement dynamics in unprecedented detail.

II. POSITRONIUM IN 1D

The Hamiltonian is given by

$$H=\frac{1}{2}p_1^2+\frac{1}{2}p_2^2+V(x_1)-V(x_2)-V(x_1-x_2). \qquad (1)$$

Positron and electron variables are denoted by 1 and 2, respectively. The electrostatic interactions are described by the soft-core Coulombic potential $V(x)=1/(x^2+1)^{1/2}$ previously used in studies involving a positive core and one or two electrons [9,10]. Our model contains two additional approximations: (i) it does not allow for positron-electron annihilation and (ii) the nucleus does not move. The first approximation is adopted in many theoretical studies of positron-atom scattering and has been justified by calculations that find that the annihilation cross section is three orders of magnitude smaller than cross sections for other inelastic channels [11]. The second approximation is obviously justified in the regime of very low incident positron kinetic energy.

Before considering the scattering problem we calculated the hydrogen and positronium eigenstates by diagonalizing the relevant two-body Hamiltonian matrix in each case, using a five-point approximation of the kinetic-energy term. The energies of the lowest states are presented in Table I and for high n the expected Rydberg behavior is found: $E_n\sim -1/n^2$. A more detailed analysis reveals that the energy relations are best understood in terms of a quantum defect such that $E_n=-R/(n+\Delta_n)^2$ [12]. The quantum defect is parity dependent since states of even parity sample more of the soft core of the potential than odd-parity states. For hydrogen it was determined that $R=2.00$ a.u. and

$$\Delta_n=\begin{cases}0.620, & n \text{ even}\\ 0.597, & n \text{ odd.}\end{cases} \qquad (2)$$

TABLE I. Binding energies for one-dimensional hydrogen and positronium eigenstates.

n	$\mathcal{B}_H$ (a.u.)	$\mathcal{B}_{Ps}$ (a.u.)
1	0.66982	0.58818
2	0.27494	0.17861
3	0.15149	0.09302
4	0.09270	0.05302
5	0.06354	0.03597
6	0.04550	0.02490
7	0.03461	0.01892
8	0.02689	0.01439
9	0.02171	0.01164
10	0.01773	0.00936

TABLE II. Final states and threshold values of free positron kinetic energy given the initial condition $e^+ + \mathrm{H}(n=1)$.

Final state	Minimum initial positron kinetic energy (a.u.)
$p + \mathrm{Ps}(n=1)$	0.082
$e^+ + \mathrm{H}(n=2)$	0.395
$p + \mathrm{Ps}(n=2)$	0.491
$e^+ + \mathrm{H}(n=3)$	0.518
$p + \mathrm{Ps}(n=3)$	0.577
$e^+ + \mathrm{H}(n=4)$	0.577
⋮	⋮
$e^+ + e^- + p$	0.670

For positronium $R = 1.00$ a.u. and

$$\Delta_n = \begin{cases} 0.340, & n \text{ even} \\ 0.274, & n \text{ odd.} \end{cases} \tag{3}$$

The agreement between the quantum-defect-modified Rydberg relation and the numerically calculated energies increases with n. Even at $n=2$ they differ by no more than 6% and by $n=10$ they agree to within 0.07%.

III. POSITRON-HYDROGEN SCATTERING DYNAMICS

The evolution of the electron-positron system is determined by the time-dependent Schrödinger equation (in dimensionless atomic units)

$$i\frac{\partial \Psi(x_1,x_2,t)}{\partial t} = H\Psi(x_1,x_2,t). \tag{4}$$

with H given in Eq. (1). In our numerical experiments the initial state consists of the electron bound to the proton in the hydrogen ground state and the positron in a Gaussian packet,

$$\psi_{e^+}(x_1, t=0) = \exp[-(x_1-x_0)^2/4\sigma^2]\exp[ik_0 x_1], \tag{5}$$

propagating towards the hydrogen atom. A typical choice of packet width was $\sigma = 30$ a.u., giving $\Delta E \approx 0.02$ a.u. for initial kinetic energies up to 1 a.u. Solutions of the time-dependent Schrödinger equation, given this initial condition, were found numerically on a spatial grid using a split-operator fast Fourier transform method described in detail elsewhere [13,14].

Our primary interest in this series of scattering experiments was to study the process of positronium formation, especially in the regime where the initial kinetic energy of the positron is from 0.082 a.u. to 0.670 a.u. In this energy regime there are several competing inelastic channels: excitation of hydrogen and the formation and possible excitation of positronium. The threshold values of initial positron kinetic energy for which these channels become open are presented in Table II. The time dependence of this scattering event is of particular interest as it has not been studied previously.

Several methods have been applied to the visualization of the collision process and will be briefly described. The first of these methods is to plot the two-particle spatial density

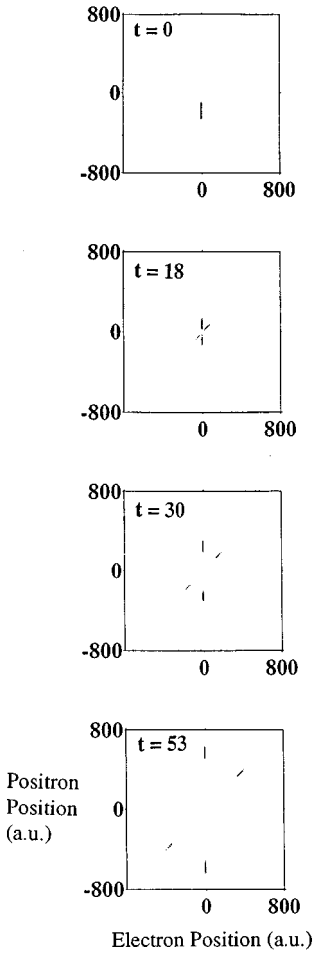

FIG. 1. Two-particle spatial density $|\Psi(x_1,x_2)|^2$ in four subsequent time frames (top to bottom) during a collision. Initially the electron is in the $\mathrm{H}(n=1)$ state and the positron is free with a kinetic energy of 0.42 a.u. The positron coordinate x_1 is along the vertical axis and the electron coordinate x_2 is along the horizontal axis. We have used a unit of time based on the frequency of the positronium 1-2 transition such that time is given in multiples of $2\pi/0.409$ a.u.

$|\Psi(x_1,x_2;t)|^2$, as shown in Figs. 1 and 2. For scattering events in which the positron's initial kinetic energy is below 0.670 a.u. (the three-body dissociation threshold) the plots have a high contrast between free positron plus hydrogen (vertical lines centered about $x_2=0$) and free proton plus positronium (diagonal lines along $x_1 \approx x_2$). The primary drawback of this method is difficulty in distinguishing between various bound states of hydrogen and positronium. Figure 1 shows a sequence of density plots of $|\Psi(x_1,x_2;t)|^2$ corresponding to different times during a scattering event. This same information for the first two plots in the sequence is shown magnified and in the format of contour plots in Fig. 2.

Greater clarity can sometimes be achieved by constructing the single-particle densities. The total electron and positron spatial densities are defined by

$$\rho_i(x_i,t) = \int_{-\infty}^{+\infty} |\Psi(x_i,x_j;t)|^2 dx_j. \tag{6}$$

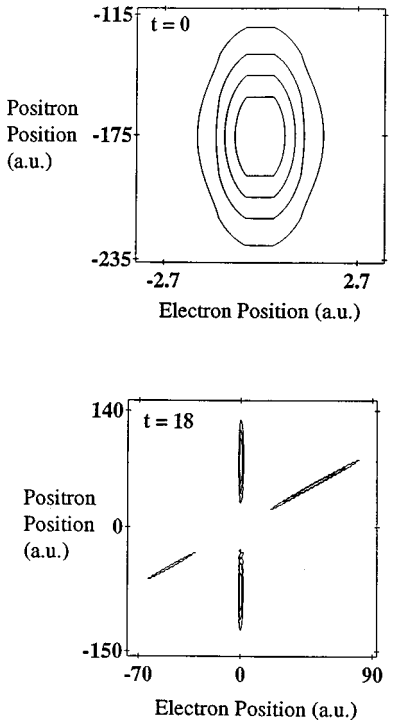

FIG. 2. Two-particle spatial density $|\Psi(x_1,x_2)|^2$ in two subsequent time frames during a collision. The contours for the $t=0$ plot are at 0.001, 0.002, 0.003, and 0.004. The contours for the $t=18$ plot are at 0.0004, 0.0007, and 0.001. Time is given in multiples of $2\pi/0.409$ a.u.

A positronium spatial density can be estimated by assuming that all $\Psi(x_1,x_2)$ for which $|x_1-x_2|\leqslant 15$ a.u. represents positronium. This approach to computing positronium density, while not rigorous, was found to be in rough agreement with more formal calculations (except in the region immediately surrounding the proton) and is considerably more efficient computationally. The free-positron density was found by subtracting this positronium density from the total positron density defined by Eq. (6). In Fig. 3 the positronium and free-positron densities are plotted for the scattering event shown in Fig. 2.

IV. INELASTIC CHANNELS

In order to gain a better understanding of the scattering process it is necessary to distinguish between the various inelastic channels that are available. A method that is better able to discern different bound states is to plot the two-particle momentum density $|\tilde{\Psi}(k_1,k_2;t)|^2$, which is found by taking the two-dimensional Fourier transform of the wave function:

$$\tilde{\Psi}(k_1,k_2)=\int\int dk_1 dk_2 \exp[i(k_1x_1+k_2x_2)]\Psi(x_1,x_2). \tag{7}$$

In a plot of the momentum density, as in Fig. 4, hydrogen bound states appear as horizontal lines at a vertical position that gives the momentum of the corresponding free positron. Measurement of this momentum plus knowledge of the binding energies enables us to identify the various lines with

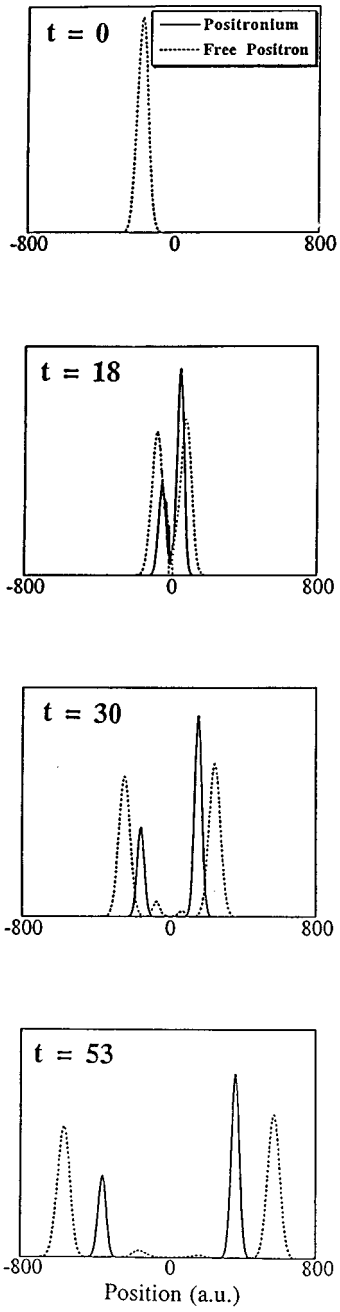

FIG. 3. Free positron and positronium spatial densities $\rho(x)$ in four subsequent time frames (top to bottom) during a collision. Initially the electron is in the H($n=1$) state and the positron is free with a kinetic energy of 0.42 a.u. Time is given in units of $2\pi/0.409$ a.u.

corresponding states through simple application of energy conservation. Similarly, the diagonal lines fall along $k_1+k_2\approx\pm K$, where K is the total momentum predicted for the various states of positronium given the initial conditions. However, our ability to distinguish between various states using this approach is limited since the spatial extent of the bound states in both position and momentum space increases with n, making it useful only for H($n=1,2$) and Ps($n=1,2$).

Numerical estimates of positronium formation cross sections for the lowest two states were found using a slight modification of momentum density method. Before taking

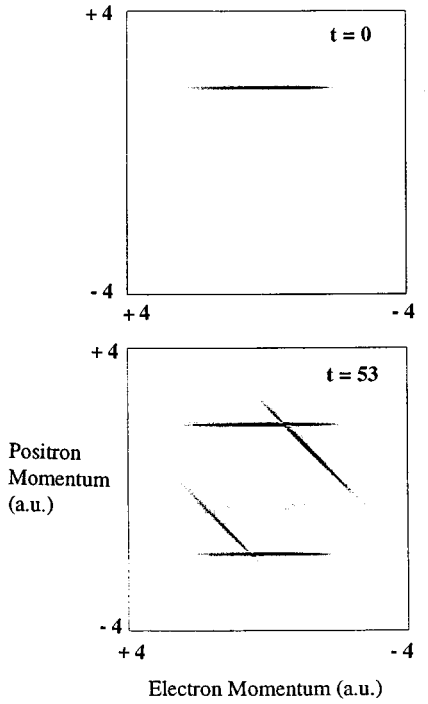

FIG. 4. Initial and final momentum distributions $|\tilde{\Psi}(k_1,k_2)|^2$ for the collision shown in Fig. 1. The positron wave vector k_1 is along the vertical axis and the electron wave vector k_2 is along the horizontal axis.

the Fourier transform a mask was applied to eliminate hydrogen from the wave function, giving a plot with clearly separated diagonal lines as shown in Fig. 5. An estimate of the probability to form positronium in a particular state can be found by summing $|\chi(k_1,k_2)|^2$ in the region for which $k_1+k_2 \approx \pm K$, where $\chi(k_1,k_2)$ is the Fourier transform of the masked wave function. We will refer to this as the mask-transform method.

Finally, a more formal approach can be used to obtain cross sections for Ps(n) formation as a function of the Ps kinetic energy. Writing the wave function in terms of hydrogen bound states $\xi_n(x_2)$ and positronium bound states $\phi_n(x_2-x_1)$ we get

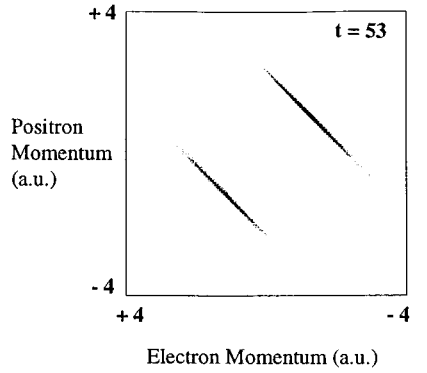

FIG. 5. Final momentum distribution $|\chi(k_1,k_2)|^2$ after applying a spatial mask to eliminate hydrogen. This plot is the masked version of Fig. 4(b).

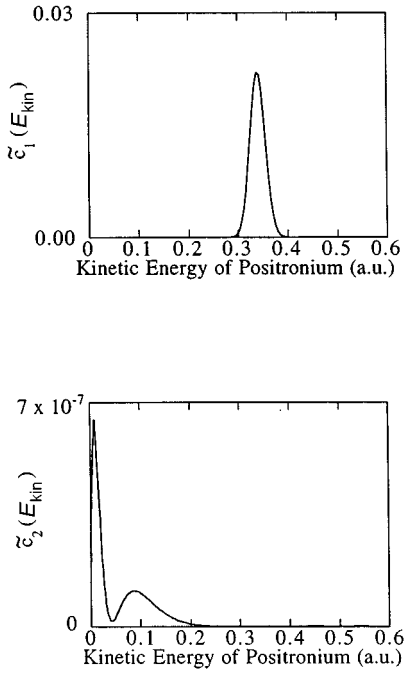

FIG. 6. Cross sections for the formation of positronium in the $n=1$ and $n=2$ states with kinetic energy (E_{kin}).

$$\Psi(x_1,x_2)=\sum_{n=1}^{\infty}\int dk b_n(k)\xi_n(x_2)\frac{1}{\sqrt{2L}}e^{ikx_1} + \sum_{n=1}^{\infty}\int dk c_n(k)\phi_n(x_2-x_1)\frac{1}{\sqrt{2L}}e^{ik(x_1+x_2)}. \tag{8}$$

Since hydrogen and positronium states are not orthogonal this expansion breaks down in the region where x_1 is small (near the proton). However, since the positron is repelled by the proton there is only a brief portion of the collision during which there is a significant amount of the wave function in this region. Therefore,

$$c_n(k)\approx\int\int dr dR\,\phi_n(r)e^{-2ikR}\Psi(r,R), \tag{9}$$

where $r=x_2-x_1$ and $R=(x_1+x_2)/2$. This method provides the most complete and accurate information about positronium formation, but at a high computational expense. $c_1(k)$ and $c_2(k)$ were computed at the final time in the scattering event shown above. In Fig. 6 we plot the corresponding kinetic-energy-dependent quantity $\tilde{c}_n(E_{kin})$, where

$$\tilde{c}_n(E_{kin})=|c_n(+\sqrt{E_{kin}})|^2+|c_n(-\sqrt{E_{kin}})|^2. \tag{10}$$

The peak in the plot of $\tilde{c}_1(E_{kin})$ is located at a positronium kinetic energy E_{kin} of approximately 0.34 a.u., which is the value predicted from conservation of energy considerations. Since the kinetic energy of the incident positron is peaked

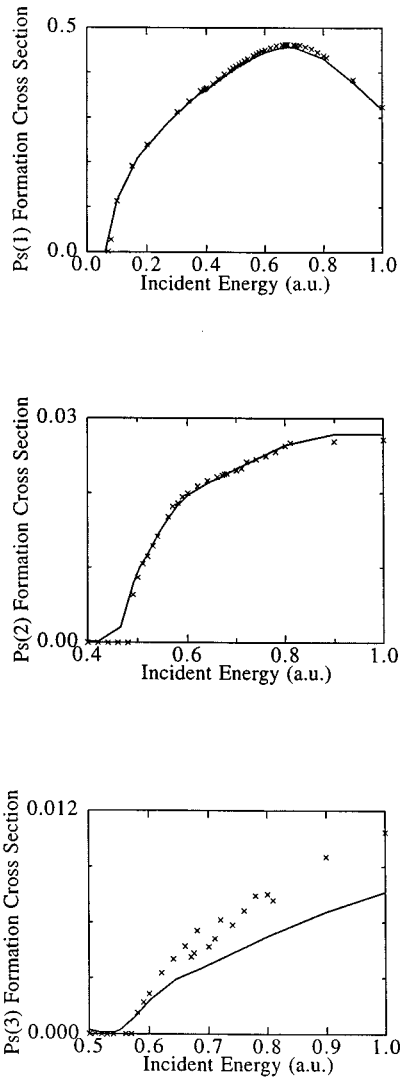

FIG. 7. Positronium formation cross sections as a function of the kinetic energy of the incident positron. The cross section found using the projection method is labeled by the solid line and that found using the mask-transform method is denoted by $\times$.

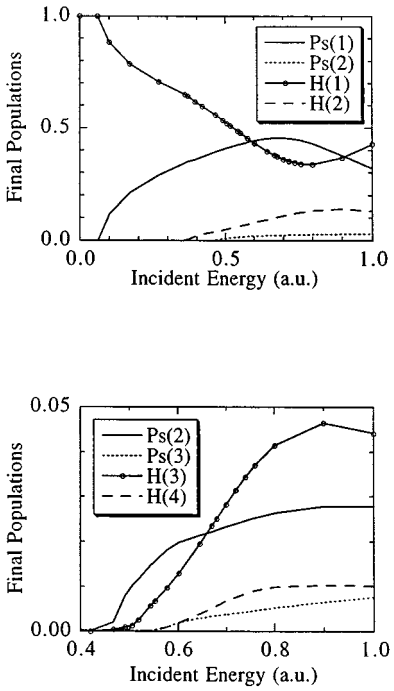

FIG. 8. Final populations in the lowest states of hydrogen and positronium as a function of the kinetic energy of the incident positron.

around 0.42 a.u. we expect little or no production of positronium in the first excited state, which is confirmed by the low values of $\tilde{c}_2(E_{\rm kin})$. The structure in the $\tilde{c}_2(E_{\rm kin})$ plot in the vicinty of 0.1 a.u. is not well understood at this time.

The population in the state n can be computed by integrating $|c_n(k)|^2$ over all k. We will refer to this as the projection method. A comparison between the mask-transform method for calculating positronium cross sections and the more rigorous projection method is shown in Fig. 7. As noted previously, the mask-transform method is not capable of accurately measuring states for which $n \geqslant 3$. However, the agreement between the methods at the lower states is quite good. In Fig. 8 we show the final populations as a function of the kinetic energy of the incident positron, calculated by the projection method. The maximum production of ground-state positronium occurs for an incident positron with 0.68 a.u. of kinetic energy, which is slightly above the three-body dissociation threshold. Our one dimensional model has a maximum production of positronium in state $n=3$ and below at an incident energy of 0.70 a.u., which is 4.5% above the dissociation energy. Experimental measurements of the total positronium formation cross section made by Sperber *et al.* [7] found a maximum at 15 ± 2.8 eV. This maximum is located 10.3% above the dissociation energy (13.6 eV).

Finally, we should note that one can justify the one-dimensional model by observing the degree of qualitative agreement with experimental data and other calculations that can be found in [8]. For example, our Ps($n=1$) cross section of Fig. 7 seems to have the same maximum as in Fig. 2(a) of Ref. [8]. The other cross sections have similar features.

V. SUMMARY

In this paper we have presented several tools for studying the one-dimensional analog of positron-hydrogen scattering. The expansion into positronium bound states in the difference coordinate and plane waves in the sum coordinate is of particular interest since it can be used in the study of nonconservative systems, unlike some of the other methods described earlier in this paper. The nonconservative laser-assisted positron-hydrogen scattering process can be studied with special emphasis on enhancement of the positronium formation cross section.

ACKNOWLEDGMENTS

We would like to thank M. Kalinski, C. K. Law, and Q. Su for their assistance throughout this project. Financial support was provided by NSF Grants Nos. PHY95-11582 and PHY96-31245. Computing resources were granted by the Pittsburgh Supercomputing Center.

[1] R. K. Pathak, Phys. Rev. A **49**, 5100 (1994).
[2] I. Aronson, C. J. Kleinman, and L. Spruch, Phys. Rev. A **4**, 841 (1971).
[3] H. S. W. Massey and C. B. O. Mohr, Proc. R. Soc. London, Ser. A **67**, 695 (1954).
[4] For a review of work up to 1985, see J. W. Humberston, Adv. At. Mol. Phys. **22**, 1 (1986).
[5] A. I. Akhiezer and N. P. Merenkov, J. Phys. B **29**, 2135 (1996).
[6] J. W. Humberston, P. Van Reeth, M. S. T. Watts, and W. E. Meyerhof, J. Phys. B **30**, 2477 (1997).
[7] W. Sperber, D. Becker, K. G. Lynn, W. Raith, A. Schwab, G. Sinapius, G. Spicher, and M. Weber, Phys. Rev. Lett. **68**, 3690 (1992).
[8] Ann A. Kernoghan, D. J. R. Robinson, Mary T. McAlinden, and H. R. J. Walters, J. Phys. B **29**, 2089 (1996).
[9] Q. Su and J. H. Eberly, Phys. Rev. A **44**, 5997 (1991).
[10] M. S. Pindzola, D. C. Griffin, and C. Bottcher, Phys. Rev. Lett. **66**, 2305 (1991); R. Grobe and J. H. Eberly, *ibid.* **68**, 2905 (1992).
[11] J. W. Humberston, Adv. At. Mol. Phys. **15**, 101 (1979).
[12] R. Loudon, Am. J. Phys. **27**, 649 (1959).
[13] R. Grobe and J. H. Eberly, Phys. Rev. A **48**, 4664 (1993).
[14] D. G. Lappas, R. Grobe, and J. H. Eberly, Phys. Rev. A **54**, 3042 (1996); D. G. Lappas, Ph.D. thesis, University of Rochester, 1995 (unpublished).